Submitted to the 29th International Conference on High-Energy Physics ICHEP98,
Vancouver, Canada, July 1998

Inclusive J/ψ Production in Deep Inelastic Scattering at HERA

H1 Collaboration

Abstract

Results on inclusive electroproduction of J/ψ mesons are presented, using the leptonic decay of J/ψ in the kinematic region of $2 < Q^2 < 80$ GeV^2 and $40 < W < 180$ GeV, where Q^2 is the negative squared four momentum transferred and W the mass of the final state hadronic system. The inclusive cross section in this kinematic region is measured to be $\sigma(ep \to e\ J/\psi\ X) = 1.35 \pm 0.27$ nb. The differential cross sections are evaluated as functions of Q^2, the transverse momentum of the J/ψ, its elasticity and the rapidity in the centre of mass frame of the virtual photon and proton. The fully inclusive distributions and also those for the "inelastic" region are compared to a leading order calculation within the non-relativistic QCD factorization approach including colour singlet and colour octet contributions. While the predictions including colour octet contributions give the correct order of magnitude of the cross sections the shape of the data is not well described.

Abstract: 573
Parallel sessions: 7,5
Plenary sessions: 9,7

1 Introduction

An analysis of inclusive J/ψ production is presented in deep inelastic positron proton scattering at a centre of mass energy of 300 GeV covering four momentum transfers of $2 \leq Q^2 \leq 80$ GeV^2. J/ψ production at HERA has previously been measured in photoproduction where the emphasis was on the one hand on data in the diffractive processes and their understanding in the framework of perturbative QCD [1, 2]. On the other hand inelastic processes [1, 3, 4] were discussed where the $c\bar{c}$ state is produced via boson gluon fusion. The data were confronted with the Colour Singlet Model [5] which had been calculated in perturbative QCD in leading and next to leading order [6] for photoproduction. The ultimate goal is a determination of the gluon density of the proton.

Measurements of the inclusive production of J/ψ in hadronic collisions [7] have shown that the Colour Singlet Model cannot account for the cross section, but a good description of the data can be achieved using a factorization approach within NRQCD [8]. In order to shed further light on the production process we present a fully inclusive analysis, for which $0.2 \leq z \leq 1$, where z is the ratio of the energies of the J/ψ and of the exchanged photon in the proton rest frame. The differential cross sections are compared to calculations of lepton proton scattering in leading order performed in the NRQCD formalism [9]. Boson gluon fusion is still the dominant production mechanism but the $c\bar{c}$ pair is produced in colour singlet and also colour octet states. The transition to the J/ψ proceeds via emission of soft gluons described by non-perturbative long range matrix elements which are presently not calculable but are expected to be universal.

In the electroproduction of charmonium the colour octet contributions are expected to dominate the cross sections, if the non-perturbative long range matrix elements determined from CDF data are used. Unfortunately the colour octet contributions are expected in approximately the same region of phase space as occurs diffractive scattering. Since diffraction is not included in the calculations an attempt at selecting non-diffractive data but keeping the colour octet contributions is made in a next step and again compared to the calculations.

2 Data and Kinematics

Data Selection Data from the years 1995 to 1997 are used where positrons of 27.5 GeV collided with protons of 820 GeV in HERA. The corresponding integrated luminosity is 21pb^{-1}. A description of the H1 detector can be found in [10]. The J/ψ event selection is briefly summarized:

- A scattered positron of energy $E > 12$ GeV is detected in an electromagnetic calorimeter (SPACAL) in an angular range of[1] $155° \lesssim \theta_e \lesssim 177.1°$. The scattered positron also provides the trigger for the events.
- Longitudinal momentum balance is required by demanding: $\delta = \sum_{all}(E - p_z) > 45$ GeV. The sum runs over *all* particles observed. For events where only particles are lost in the proton direction $\delta \approx 2\,E_e$ where E_e is the energy of the incoming positron.

[1]The polar angle is measured relative to the proton direction.

- Two identified muons or electrons of opposite charge coming from the nominal interaction region are required with polar angles within $20° \leq \theta \leq 160°$. Their transverse momenta have to satisfy $p_t > 0.8$ GeV. The particles are measured in the central tracking detector. Electrons are identified in the electromagnetic LAr calorimeter. Muons are identified either in the muon detector (instrumented iron return yoke of the magnet) or as minimum ionizing particles in the calorimeter.

- Additional particles observed in the tracking detectors and/or the calorimeters are allowed.

The mass spectra are displayed in fig. 1 in bins of z for muon and electron decays separately. A clear J/ψ signal is observed for values of $z \gtrsim 0.35$, the position and width of which agree with expectations. The signal-to-background ratio is found to depend mainly on z. Therefore the number of signal events is determined in bins of z in the following way: all events in a mass region of ± 250 MeV around the nominal J/ψ mass are counted. In order to subtract the non-resonant background each event is given a weight $(1 - f_{NR})$, where $f_{NR}(z)$ is the background probability. It is obtained from fitting the background by a power law m^{-n}.

Note that contributions from $\psi(2S)$ are included in the selection as are possible other decays which result in a J/ψ.

Reconstruction of Kinematics The $e\Sigma$ [11] method is used for reconstructing the event kinematics, which uses the scattered positron *and* the hadronic final state. The variable $Q^2 = -q^2 = -(k - k')^2$, where k and k' are the four vectors of the incoming and scattered positron, is reconstructed from the scattered positron. For the calculation of $y = (q \cdot p)/(k \cdot p)$ and $z = (p_\psi \cdot p)/(q \cdot p)$ (p denotes the four vector of the incoming proton) the observed final state is used in addition. Thus

$$y = \frac{\sum_{had}(E - p_z)}{\sum_{all}(E - p_z)} \quad \text{and} \quad z = \frac{(E - p_z)_\psi}{\sum_{had}(E - p_z)},$$

where the sum indicated by "had" runs over all particles observed in the final state but excluding the scattered positron. The resolution in the variables Q^2, $p_{t,\psi}^2$ and y^*, the rapidity of the J/ψ in the $\gamma^* p$ centre of mass, is good $(2 - 5\ \%)$. For z the resolution is good at high z and degrades towards low z, it is on average $17\ \%$ for $z < 0.9$.

Using the $e\Sigma$ reconstruction method radiative corrections are calculated to be $6 - 8\ \%$ [12].

Data Correction Acceptance and efficiencies are corrected using a simulation tailored to describe the data, i.e. the diffractive portion is described by the generator DIFFVM [13] and the inelastic portion by EPJPSI [14], which generates events according to the Colour Singlet Model. Both models were previously shown to describe diffractive and inelastic data respectively. For the present inclusive analysis the normalization of EPJPSI was determined in the region $0.4 < z < 0.8$ and DIFFVM was added to describe the data at $z > 0.95$. Extensive checks were carried out to ensure that all important aspects of the data are well described by this mix. A few comparisons are shown in fig. 2. The reconstruction efficiencies of tracks and the identification efficiencies for leptons in the simulation were optimized using independent lepton data. The reconstruction and triggering efficiencies are of the order $60\ \%$ in the chosen kinematic region.

The branching ratios for $J/\psi \to \mu^+\mu^-$ and $J/\psi \to e^+e^-$ are $6.01 \pm 0.19\ \%$ and $6.02 \pm 0.19\ \%$, respectively [15].

3 Theory

Fleming and Mehen [9] calculated the production cross sections within the NRQCD factorization approach, where the ep cross section is written as a sum:

$$\sigma(e + p \rightarrow e + J/\psi + X) = \sum_n c_n(e + p \rightarrow e + c\bar{c}[n] + X)\langle \mathcal{O}_n^{J/\psi} \rangle,$$

where n denotes an on-shell $c\bar{c}$ pair in a definite colour, spin and angular momentum state. For each n, the cross section factorizes into a short distance part c_n calculable in a perturbative QCD expansion in α_s and a long distance matrix element $\langle \mathcal{O}_n^{J/\psi} \rangle$ giving the probability for the $c\bar{c}$ pair in the state n to transform into a J/ψ meson. The long range matrix elements will be written in spectroscopic notation: $\langle \mathcal{O}_{(1,8)}(^{2S+1}L_J) \rangle$, where the subscripts (1) or (8) refer to the colour configuration of the $c\bar{c}$ system, i.e. colour singlet and colour octet respectively.

The calculation includes the types of diagrams of order α_s shown in figure 3a) and b) and of order α_s^2 (figure 3c). The Colour Singlet Model in leading order includes only diagrams of type fig. 3c). Fleming and Mehen estimate the calculations to be reliable for $Q^2 > 4$ GeV^2.

The predicted differential cross sections $d\sigma/dQ^2$ for the production of J/ψ mesons in deep inelastic ep scattering at HERA, including the contributions from the colour octet states $^3P_0$, $^1S_0$ and the colour singlet state $^3S_1$, are shown in figure 4 for the kinematic region $40 < W < 180$ GeV, using GRV(LO) [16] parton densities. The sum of the colour octet contributions dominates the cross section for all Q^2. Since the octet $^3P_0$ and $^1S_0$ contributions have a similar shape, the cross section is only sensitive to a linear combination of the two corresponding matrix elements. The following values for the long distance matrix elements have been used in the calculations shown in figure 4:

$$\langle \mathcal{O}_{(1)}(^3S_1) \rangle = 1.1 \text{ GeV}^3; \quad (1)$$

$$\langle \mathcal{O}_{(8)}(^1S_0) \rangle = 0.01 \text{ GeV}^3; \quad (2)$$

$$\langle \mathcal{O}_{(8)}(^3P_0) \rangle / m_c^2 = 0.005 \text{ GeV}^3. \quad (3)$$

Note that these values are considered order of magnitude estimates [9]. The singlet matrix element is determined — in analogy to the Colour Singlet Model — from the measured electronic decay width of the J/ψ.

Colour octet contributions to J/ψ production are in leading order in α_s predominantly expected at large z. This is because the $c\bar{c}$ pair can be produced with no other particles in the final state, i.e. $z \approx 1$. The non-perturbative transition into the J/ψ meson reduces the value of z only slightly. Experimentally, J/ψ mesons produced via colour octet states are thus expected to be kinematically very similar to diffractively produced J/ψ mesons, which also occur at large z.

4 Results

Differential Cross Sections The inclusive differential cross sections are shown in fig. 5 (open points) as functions of Q^2, $p_{t,\psi}^2$, z and y^*, the rapidity of the J/ψ in the $\gamma^* p$ centre of mass system.

A clear enhancement is visible in the data at $z \approx 1$, where diffractive and also colour octet contributions are expected. In order to suppress the diffractive processes and to retain possible octet contributions a cut is applied which suppresses low masses of the hadronic state besides the J/ψ characteristic for diffractive processes: the experimental variable which is related to the hadronic mass is the energy E_{fwd} deposited in the "forward" region of the detector, i.e. in the LAr calorimeter at polar angles of $\theta < 20\,°$. Imposing a cut $E_{fwd} > 5$ GeV suppresses the diffractive event contribution so that the remaining fraction is of the order of $6\ \%$ according to simulation. The effect of the cut can be seen in the resulting cross sections also displayed in fig. 5 (full points). Note that the data have not been corrected for a loss of non-diffractive events, which is however estimated to be below $20\ \%$.

The data are compared to the prediction by Fleming et al. as described in section 3[2]. The colour singlet contribution which is shown separately is seen to fall below the data everywhere by large factors. Including colour octet contributions the predictions come closer to the data in magnitude, but the shapes are different. This is in particular true for y^*.

In previous analyses different methods were used to define the inelastic region, such as demanding additional activity in the detector or applying a cut $z < 0.9$. We have tried these methods also without significant change in the conclusions.

As a last comparison, the lower limit on Q^2 is raised to 3.7 GeV^2, at the same time requiring $p_{t,\psi}^2 > 3.4$ GeV^2 in order to come closer to the regime where the theory is considered reliable. In fig. 6 the data for $E_{fwd} > 5$ GeV are compared to the calculation. The conclusions do not change significantly from those based on fig. 5.

Integrated Cross Sections The inclusive ep cross section in the kinematic region $2 < Q^2 < 80$ GeV^2 and $40 < W < 180$ GeV is determined to be:

$$\sigma(ep \to e\ J/\psi\ X) = 1.35 \pm 0.10(\text{stat.}) \pm 0.25(\text{syst.})\ \text{nb.}$$

The systematic error is dominated by uncertainties in analysis efficiencies and the method of subtraction of non-resonant background. The direct measurement of the diffractive cross section in a similar kinematic region [17] yields approximately $45\ \%$ of this number.

Applying the cut $E_{fwd} > 5$ GeV in order to suppress diffractive contributions yields in the same kinematic range as above:

$$\sigma(ep \to e\ J/\psi\ X) = 0.63 \pm 0.09(\text{stat.}) \pm 0.12(\text{syst.})\ \text{nb.}$$

Decay Angular Distributions Measuring the polarization of the J/ψ is thought to be a way of distinguishing various contributions to J/ψ production. The decay angular distributions in the helicity frame are shown in fig. 7 for the fully inclusive case and for the inelastic selection which rejects most diffractive production. It is predicted to be

$$\frac{d\,\sigma}{d\,\Omega} \propto 1 + \alpha \cos\theta^2.$$

[2]Note that the "unphysical" sharp edges in this and the following figure in the theoretical $p_{t,\psi}^2$ and y^* cross sections which include colour octet contributions are due to the kinematic cuts in Q^2 and W and due to the fact that effects of the non-perturbative transition to the J/ψ are not considered for colour octet states.

For J/ψ production via the colour singlet mechanism $\alpha \approx 0.5$ is expected [18]. If colour octet contributions are present $|\alpha| \lesssim 0.5$, where α can be negative, zero or positive depending on which intermediate $c\bar{c}$ state dominates in the production.

The data yield values of 0.35 ± 0.30 for the inclusive case and $0.57^{+0.49}_{-0.40}$ for the inelastic selection (compare: $\alpha = 0.26^{+0.36}_{-0.30}$ for $z > 0.9$, the diffractive regime). The uncertainties are still too large for definitive conclusions.

5 Discussion

Data have been presented for the inclusive production of J/ψ mesons in deep inelastic scattering. Using a selection cut which suppresses events with a low mass hadronic system, diffractive events are removed.

A leading order calculation in the NRQCD factorization approach is confronted with our measurements of differential cross sections. Rough agreement in magnitude is found, using long range matrix elements determined from Tevatron data. However the shape of the Q^2, $p^2_{t,\psi}$ and J/ψ rapidity distributions differ between data and theory. Agreement may be reached by decreasing the size of the colour octet long distance matrix elements or by including higher orders in the NRQCD perturbative expansion. Furthermore the data include a small contribution from higher mass resonances, mainly $\psi(2S)$, which are not present in the theoretical calculations.

The colour singlet contribution is below the data by large factors. Nevertheless the Colour Singlet Model alone seems to come closest to the shapes of the differential cross sections, although in particular the rapidity distribution of the J/ψ is not well described.

Raising the lower limit of Q^2 from 2 to 3.7 GeV^2 does not change these conclusions.

Acknowledgements

We are grateful to the HERA machine group whose outstanding efforts have made and continue to make this experiment possible. We thank the engineers and technicians for their work in constructing and now maintaining the H1 detector, our funding agencies for financial support, the DESY technical staff for continual assistance, and the DESY directorate for the hospitality which they extend to the non–DESY members of the collaboration. We thank S. Fleming and T. Mehen for valuable discussions and for making their theoretical predictions available.

References

[1] H1 Collaboration, S. Aid et al., Nucl. Phys. **B472** (1996) 3; H1 Collaboration, C. Adloff et al., *Elastic Production of J/ψ Mesons in Photoproduction and at High Q^2 at HERA*, contributed paper 242 to HEP 1997, Jerusalem.

[2] ZEUS Collaboration, J. Breitweg et al., Z. Phys. **C75** (1997) 215; ZEUS Collaboration, J. Breitweg et al., *Exclusive Vector Meson Production in Deep Inelastic Scattering at HERA*, contributed paper 639 to HEP 1997, Jerusalem.

[3] H1 Collaboration, S. Aid et al., *Diffractive and Non-diffractive Photoproduction of J/ψ at HERA*, contributed paper pa02-085 to ICHEP 1996, Warsaw.

[4] ZEUS Collaboration, J. Breitweg et al., Z. Phys. **C76** (1997) 599.

[5] E.L. Berger and D. Jones, Phys. Rev. **D 23** (1981) 1521;
R. Baier and R. Rückl, Phys. Lett. **B102** (1981) 364; Nucl. Phys. **B201** (1982) 1; Z. Phys. **C19** (1983) 251.

[6] M. Krämer, Nucl. Phys. **B459** (1996) 3.

[7] CDF Collaboration, F. Abe et al., Phys. Rev. Lett. **69** (1992) 3704; ibid. **79** (1997) 572;
DØ Collaboration, S. Abachi et al., Phys. Lett. **B370** (1996) 239.

[8] G.T. Bodwin, E. Braaten and G.P. Lepage, Phys. Rev. **D51** (1995) 1125, Erratum ibid. **D55** (1997) 5853;
E. Braaten and Y. Chen, Phys. Rev. **D54** (1996) 3216;
W.E. Caswell and G.P. Lepage, Phys. Lett. **B167** (1986) 437.

[9] S. Fleming and T. Mehen, Phys. Rev. **D57** (1998) 1846.

[10] H1 Collaboration, I. Abt et al., Nucl. Instr. and Meth. **A368** (1997) 310;
H1 Collaboration, I. Abt et al., Nucl. Instr. and Meth. **A368** (1997) 348.

[11] U. Bassler and G. Bernardi, Nucl. Instr. and Meth. **A361** (1995) 197.

[12] A. Arbuzov, D. Bardin, J. Bluemlein, L. Kalinovskaya and T. Riemann, *HECTOR 1.00 - A Program for the Calculation of QED, QCD and Electroweak Corrections to ep and $l^{\pm}N$ Deep Inelastic Neutral and Charged Current Scattering*, DESY Report **95-185** (1995).

[13] B. List, Diploma Thesis, Techn. Univ. Berlin, unpublished (1993).

[14] H. Jung, *The Monte Carlo Generator EPJPSI for J/ψ-Mesons in High Energy Electron Proton Collisions*, in: Proc. of the Workshop on Physics at HERA, ed. W. Buchmüller and G. Ingelman, Hamburg (1992), Vol. 3, p. 1488;
H. Jung, D. Krücker, C. Greub and D. Wyler, Z. Phys. **C60** (1993) 721.

[15] R. M. Barnett et al., Phys. Rev. **D54** (1996) 1.

[16] M. Glück, E. Reya and A. Vogt, Z. Phys. **C67** (1995) 433.

[17] H1 Collaboration, C. Adloff et al., *Diffractive Charmonium Production in Deep Inelastic Scattering at HERA*, contributed paper 572 to ICHEP 1998, Vancouver.

[18] S. Fleming, private communication (1997).

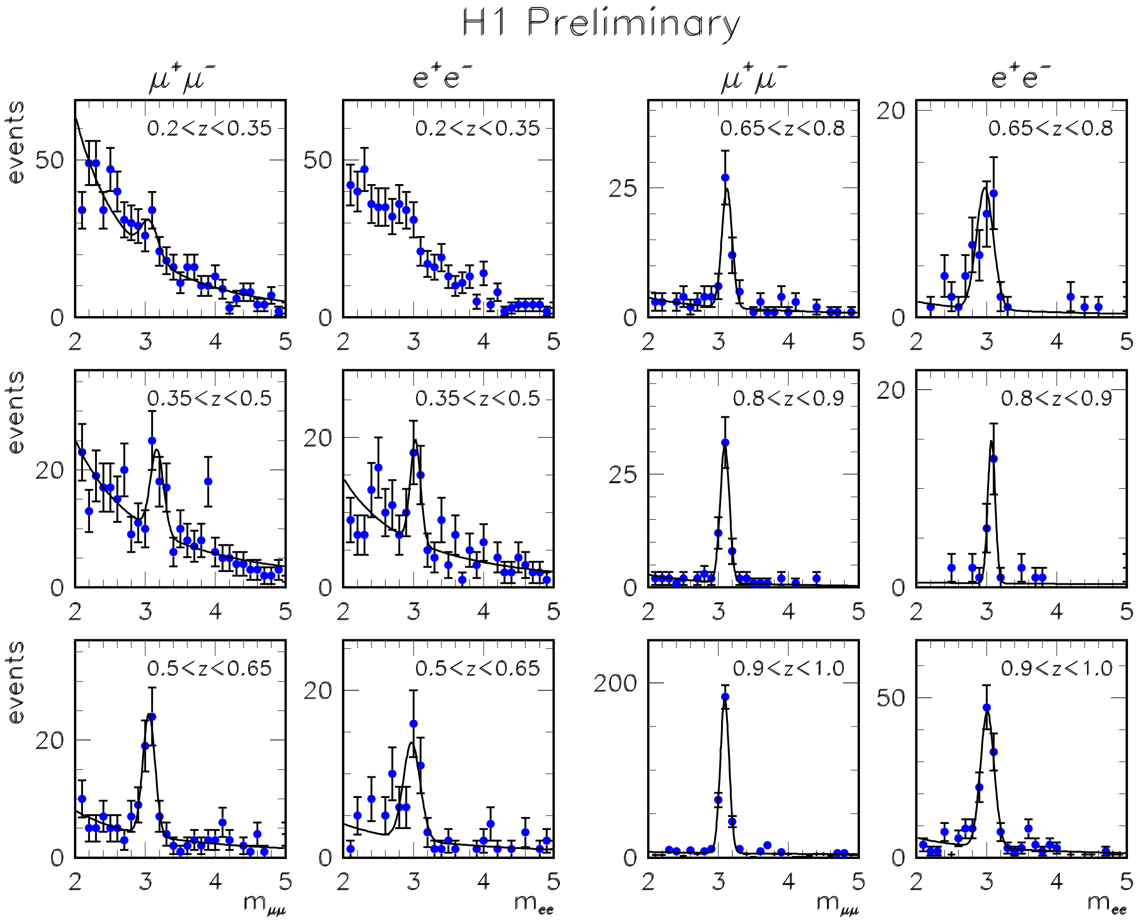

Figure 1: *Mass spectra* (GeV) *in bins of the elasticity z for the inclusive J/ψ selection for the muonic and electronic decay channels separately. The curves are fits of a Gaussian and a power law for the background.*

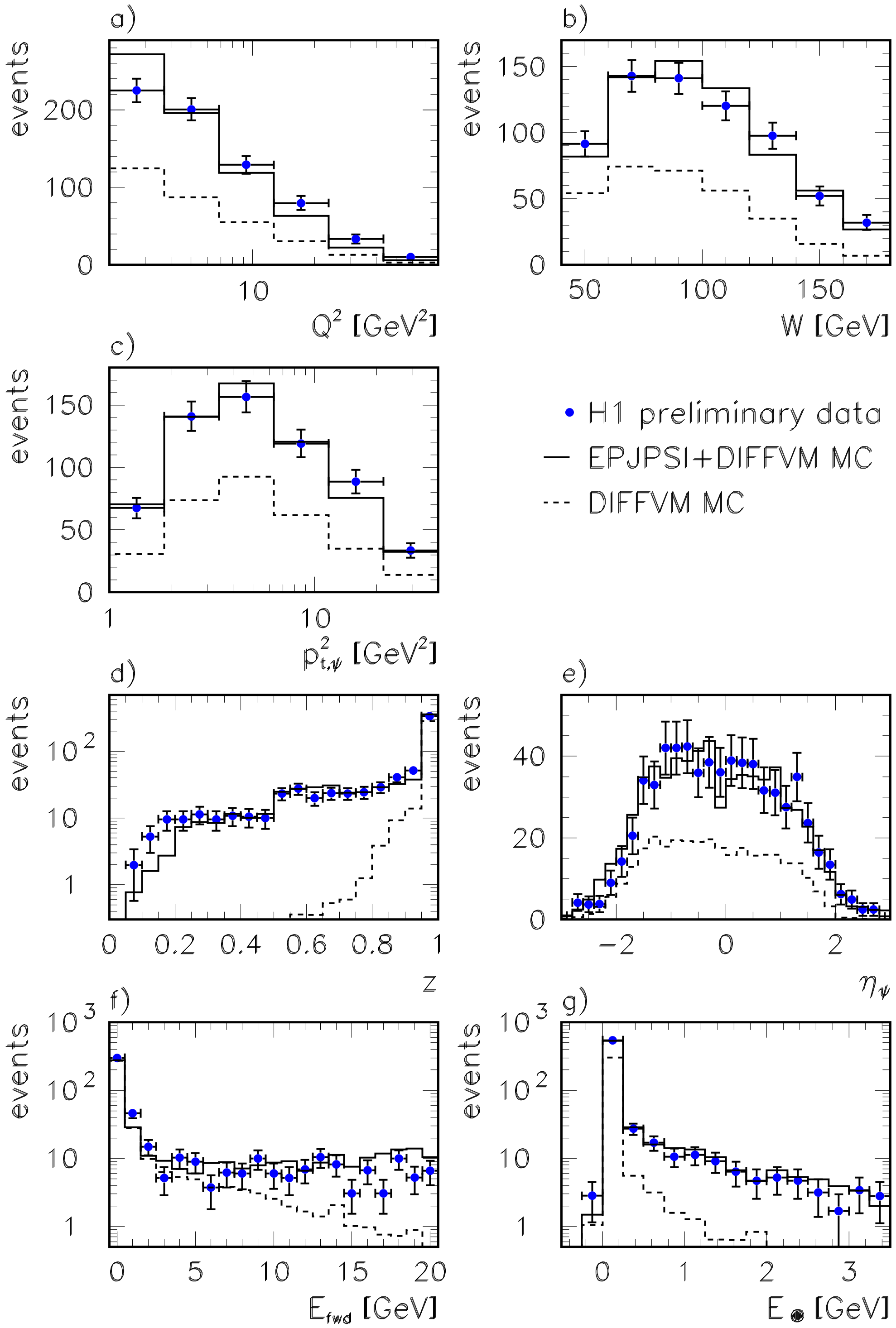

Figure 2: *Comparison between data and Monte Carlo simulation of kinematic variables for inclusive J/ψ production. a) Q^2, b) W, c) $p^2_{t,\psi}$, d) the elasticity z, e) the pseudorapidity η_ψ of the J/ψ in the laboratory frame, f) energy deposited in the LAr calorimeter for $\theta < 20°$, and g) energy in a cone with radius $R = 1$ around the J/ψ direction of flight. The data are represented by points, while the histograms show the combined (DIFFVM and EPJPSI) Monte Carlo simulation (full lines) and the DIFFVM contribution separately (dashed lines).*

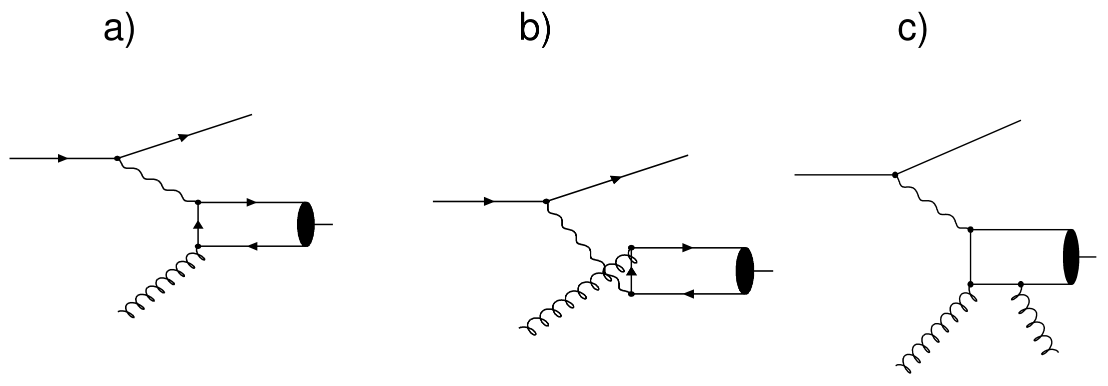

Figure 3: *Diagrams contributing to the virtual photoproduction of J/ψ at leading order in NRQCD. Diagrams of type a) and b) contribute $c\bar{c}$ pairs in colour octet states, while c) produces colour singlet states.*

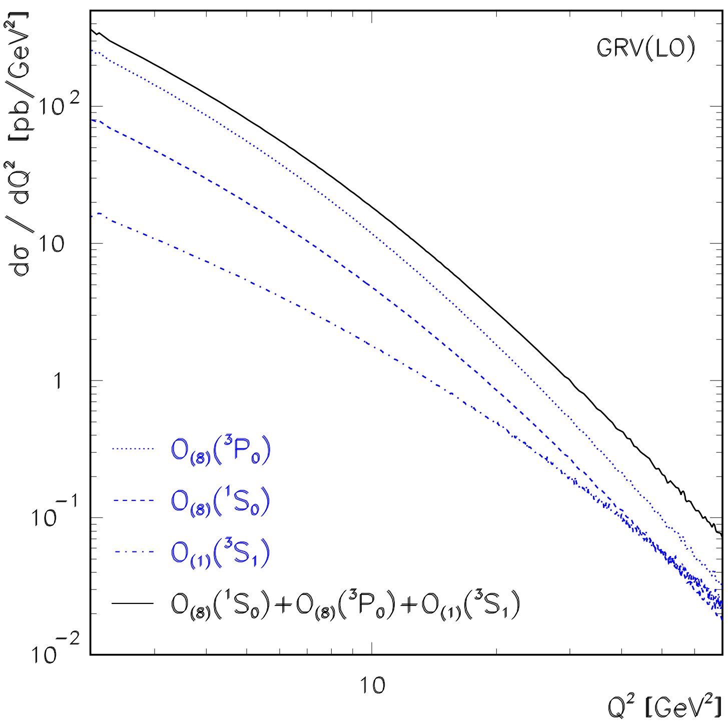

Figure 4: *Prediction by Fleming and Mehen [9] for the J/ψ virtual photoproduction cross section $d\sigma/dQ^2$ in the region $40 < W < 180$ GeV. The colour octet contributions are $\mathcal{O}(\alpha_s)$ and the colour singlet prediction is $\mathcal{O}(\alpha_s^2)$.*

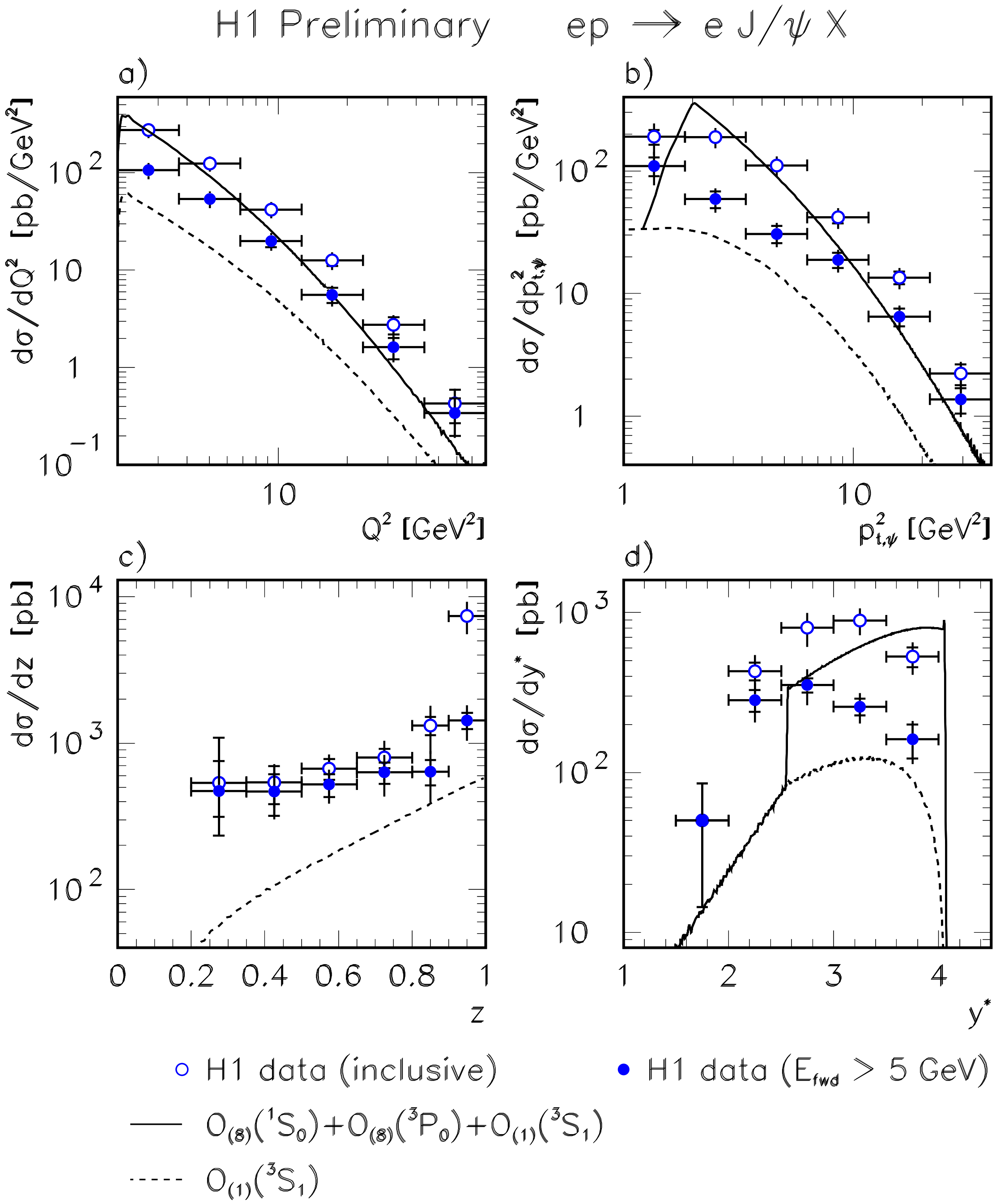

Figure 5: *Differential cross sections for the inclusive (open points) and inelastic ($E_{fwd} > 5$GeV, black points) $ep \to e\ J/\psi\ X$ process in the kinematic region of $2 < Q^2 < 80$ GeV^2 and $40 < W < 180$ GeV. a) $d\sigma/dQ^2$, b) $d\sigma/dp^2_{t,\psi}$, c) $d\sigma/dz$ and d) $d\sigma/dy^*$. Inner error bars are statistical, outer error bars statistical and systematic errors added in quadrature. The curves are predictions [9] within the NRQCD factorization approach for the colour singlet contribution and the sum of singlet and octet contributions. Note that the "unphysical" sharp edges in this and the following figure in the theoretical $p^2_{t,\psi}$ and y^* cross sections which include colour octet contributions are due to the kinematic cuts in Q^2 and W and due to the fact that effects of the non-perturbative transition to the J/ψ are not considered for colour octet states.*

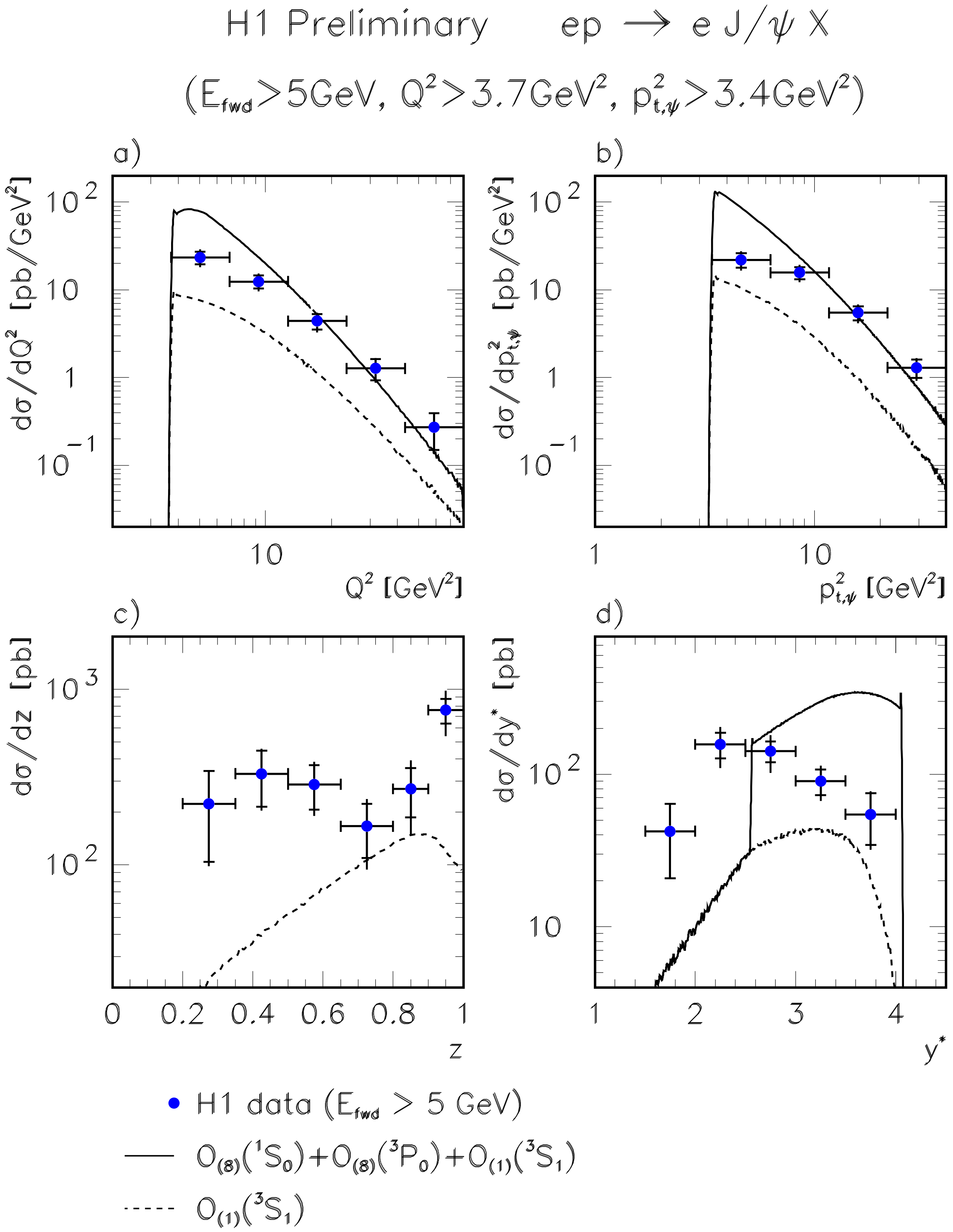

Figure 6: *Differential cross sections for $ep \to e\,J/\psi\,X$ with $E_{fwd} > 5\,$GeV, $Q^2 > 3.7\,$GeV^2 and $p^2_{t,\psi} > 3.4\,$GeV^2; a) $d\sigma/dQ^2$, b) $d\sigma/dp^2_{t,\psi}$, c) $d\sigma/dz$ and d) $d\sigma/dy^*$. The curves are predictions [9] within the NRQCD factorization approach .*

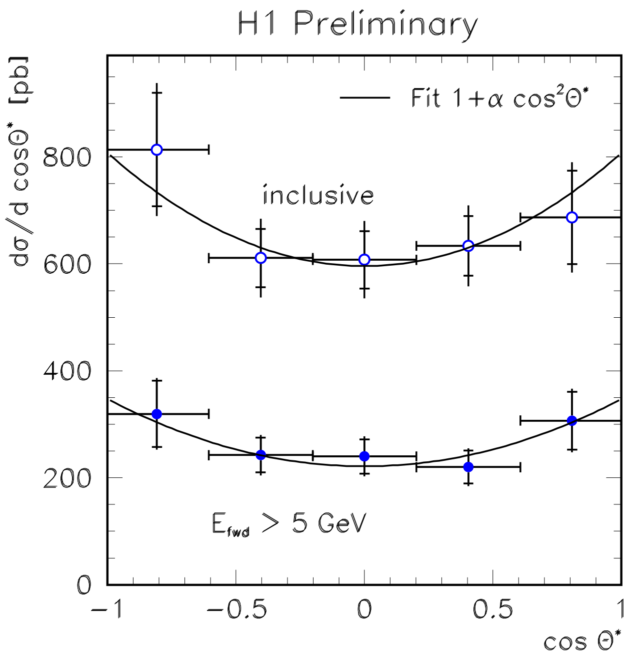

Figure 7: *Differential cross sections $d\sigma/d\cos\theta^*$ for $ep \rightarrow e\ J/\psi\ X$. The fully inclusive cross section and the inelastic cross section ($E_{fwd} > 5$ GeV) is shown. The lines are fits to the form $\sim 1 + \alpha\cos^2\theta^*$.*